Solid-State Electronics 210 (2023) 108812

Contents lists available at ScienceDirect

Solid State Electronics

journal homepage: www.elsevier.com/locate/sse

Modeling and simulation of successive breakdown events in thin gate dielectrics using standard reliability growth models

E. Miranda [a,*], F.L. Aguirre [a], E. Salvador [a], M.B. González [b], F. Campabadal [b], J. Suñé [a]

[a] Universitat Autònoma de Barcelona, 08193 Cerdanyola del Valles, Spain
[b] Institut de Microelectrònica de Barcelona, IMB-CNM, 08193 Cerdanyola del Valles, Spain

ARTICLE INFO

Handling Editor: Sorin Cristoloveanu

Keywords:
Dielectric breakdown
Oxide breakdown
MOS
MIM
Oxide reliability

ABSTRACT

The application of constant electrical stress to a metal–insulator-semiconductor (MOS) or metal–insulator-metal (MIM) structure can generate multiple breakdown events in the dielectric film. Very often, these events are detected as small jumps in the current–time characteristic of the device under test and can be treated from the stochastic viewpoint as a counting process. In this letter, a wide variety of standard reliability growth models for this process are assessed in order to determine which option provides the best simulation results compatible with the experimental observations. For the generation of the breakdown event arrivals, two alternative stochastic methods for the power-law Poisson process are investigated: first, the inversion algorithm for the cumulative distribution function and second, an on-the-fly method based on the so-called rejection algorithm. Though both methods are equivalent, the first one is more appropriate for data analysis using spreadsheet calculations while the second one is highly suitable for circuit simulation environments like LTSpice. The connection of the selected nonhomogeneous Poisson process with the Weibull model for dielectric breakdown is also discussed.

1. Introduction

Application of constant or ramped voltage/current stress to a MIM or MIS structure can generate successive breakdown (BD) events in the dielectric film that are often detected as jumps in the conduction characteristic of the device. This kind of experiment is the basis of thin oxide reliability analysis and is often carried out for assessing the integrity of the dielectric layer for a given technology. In this letter, we will exclusively focus the attention on constant voltage stress (CVS). In principle, when the number of investigated devices is large enough, the most complete information about the arrival time of successive BD events is obtained from the order statistics analysis. It has been demonstrated that the time-to-BD for the first, second, third and so on events occurring in a device subject to CVS can be succesfully modeled by the clustering distribution or alternatively, when variability is under control, by one of its limits, *i.e.* the Weibull distribution [1]. However, when the number of measurements is small and simulated curves with average features are required, a first order approach consists in considering standard reliability growth models [2]. In general, these models describe how the system reliability changes over time during the testing process and in a broad sense they are equivalent to the parametric probability distributions but for processes instead of data. Moreover, they can be identified with stochastic diffusive processes with deterministic average trends. In this work, we show the distinctive behavior exhibited by different reliability growth models (polynomial, exponential, logarithmic, power-law), discuss their pros and cons and analyze in detail the best option compatible with the experimental observations. We report two methods for the generation of succesive BD events according to a power-law Poisson process: first, the inversion algorithm for the cumulative distribution function and second, an on-the-fly method based on the so-called rejection algorithm. Though both methods provide similar results, the first one is more appropriate for data analysis using spreadsheet calculations while the second is highly suitable for circuit simulators. In this work, LTspice from Analog Devices will be considered to this purpose. We will also show how the proposed approach can be extended for simulating different generation laws other than the one specifically addressed here. This opens the path to the investigation of more complex generation process involving acceleration factors or self-regulatory mechanisms.

* Corresponding author.
E-mail address: enrique.miranda@uab.cat (E. Miranda).

https://doi.org/10.1016/j.sse.2023.108812

Available online 28 October 2023

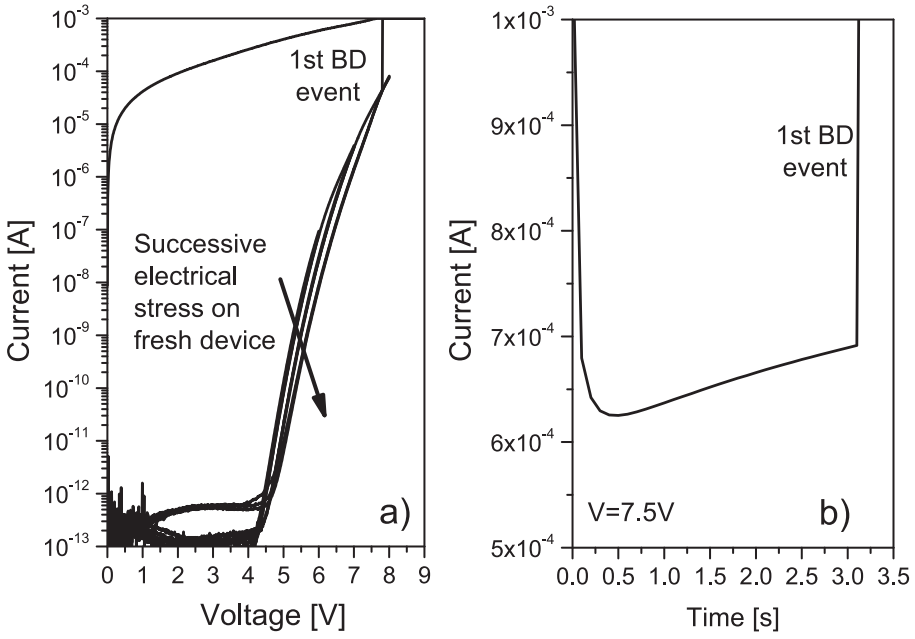

Fig. 1. a) i-v and b) i-t curves after and before the first bd event. notice the effect of electrical stress.

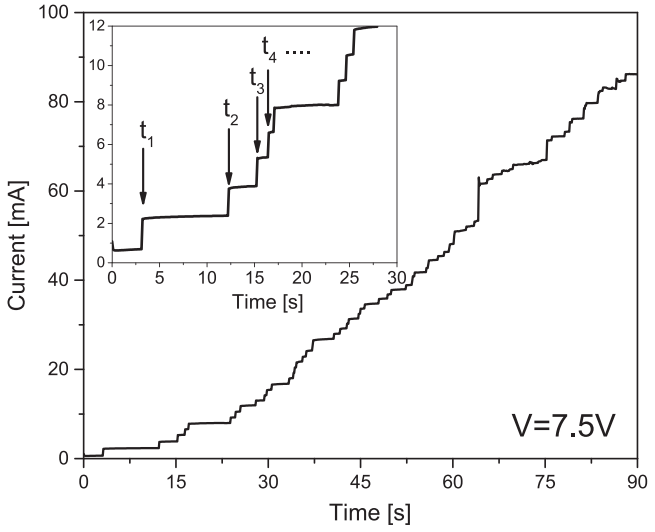

Fig. 2. Evolution of the current as a function of time for a constant applied bias (7.5 V). The inset shows a detail of the initial steps and the arrival time of the BD events.

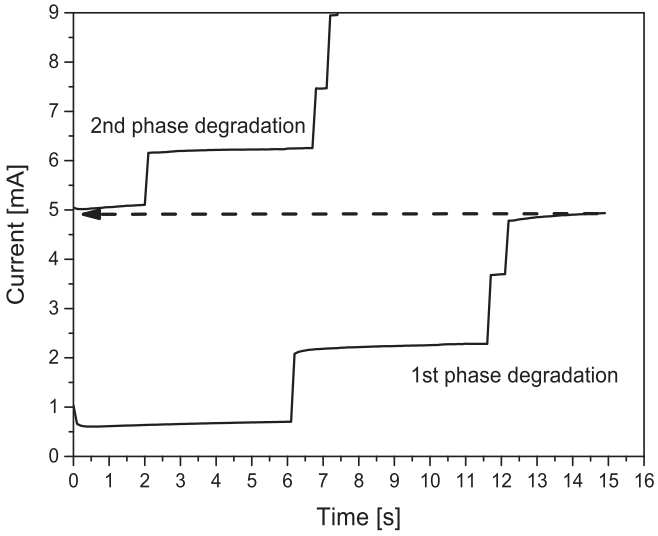

Fig. 3. Two-phase degradation showing the non-volatility character of the generated failures. The degradation was stopped for several seconds and then resumed.

2. Devices and measurements

Measurements shown in this work were obtained with Al/Al_2O_3/p-type Si capacitors. The Al_2O_3 layer was grown (10 nm-thick) by the atomic layer deposition (ALD) technique. Details about the sample fabrication, characterization and reliability characteristics can be found in [3,4]. Fig. 1.a and 1.b illustrate typical current–voltage (*I-V*) and current–time (*I-t*) curves for the device under test before and after the first BD event, respectively. As shown in Fig. 1.a, the application of successive voltage ramps with increasing maximum voltage generates electron trapping in the structure that ends with the formation of a BD path and therefore with a huge increase of the leakage current that flows through the device. This corresponds to a hard BD failure mode. In the case of Fig. 1.b, where a constant voltage is applied, the leakage current initially decreases in agreement with the results shown in Fig. 1.a, but then starts increasing, presumably because of electron traps generation, until the occurrence of the failure event.

Fig. 2 shows the staircase evolution of the current during degradation at constant voltage (7.5 V). As illustrated in the inset of Fig. 2, t_i corresponds to the BD time for event *i*. Additionally, Fig. 3 shows that the failure events are non-volatile and irreversible. In this case, the degradation was stopped ($V = 0$ V) for several seconds and then resumed. The current magnitude at the onset of the second phase corresponds to the final current magnitude of the first phase.

3. Exploratory analysis of reliability growth models

In order to deal with the stepwise behavior of the *I-t* characteristics exhibited by our devices, we consider the random arrival of BD events as a point process with $\Lambda(t)$ the number of events at time *t*. In particular, non-homogeneous Poisson processes (NHPP) with time-varying rate

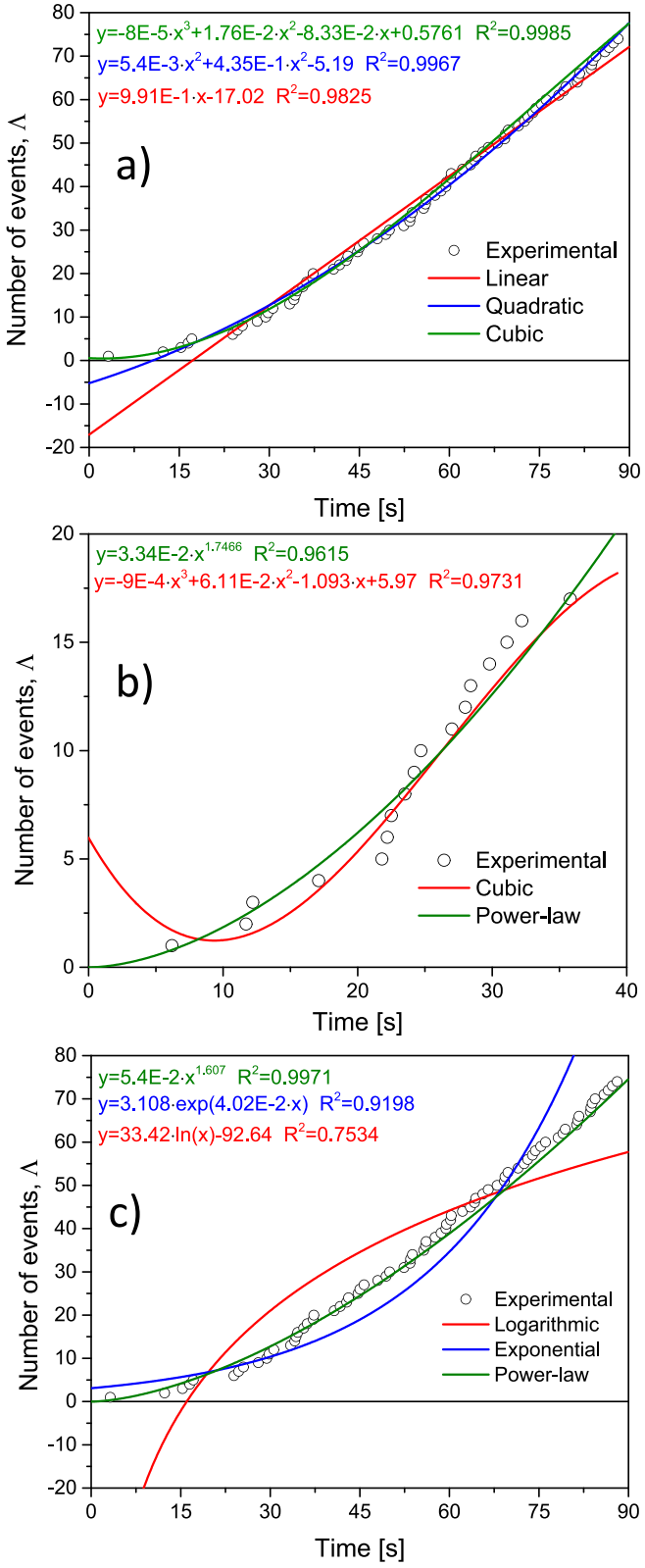

Fig. 4. Model fitting and correlation coefficients: a) polynomial, b) cubic and power-law (less datapoints corresponding to a different measurement), c) logarithmic, exponential, and power-law.

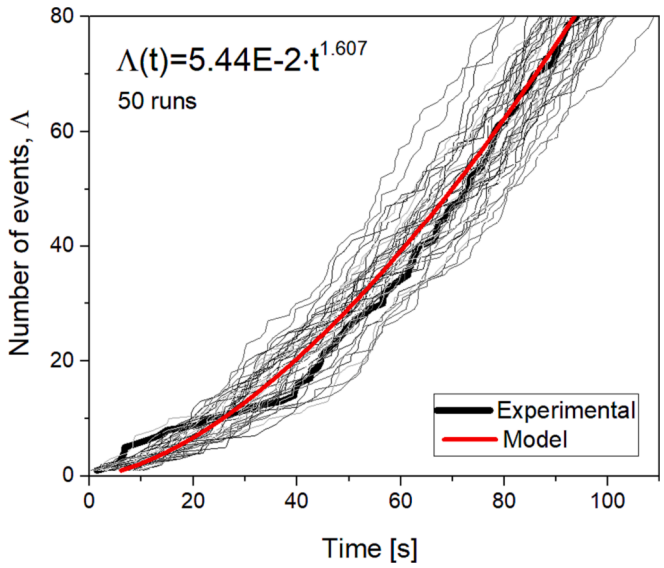

Fig. 5. inversion algorithm for the generation of bd times. b) number of events as a function of time. the grey lines corresponds to 50 runs.

function (intensity function) $\lambda(t) = d\Lambda(t)/dt$ are assumed here. Since NHPP is a Markovian process, we are implicitly assuming that the system has no memory (past events are not correlated with future events) and disjoint time intervals are independent. Six standard models are analyzed in this work as possible candidates for $\Lambda(t)$ with the aim of determining the best option for the available data set: polynomials of degree 1 to 3, exponential: $a{\cdot}\exp(b{\cdot}t)$, logarithmic: $a{\cdot}\ln(t) + b$, and power function: $a{\cdot}t^b$, the latter so-called Duane/Crow-AMSAA model or power-law process (PLP). Parameters were first extracted using the least-squares method (LSM). Notice that these models refer to the number of BD events and not directly to the current magnitude. Fig. 4.a shows fitting results with the polynomials. Clearly, the best result is obtained with the cubic expression. Linear and quadratic expressions not only depart from the experimental data but also yield negative values for the first few events. The problem with the cubic interpolation is that if not used with care it can generate unexpected results both for low and high number of events (see Fig. 4.b). This strongly depends on the number of data points considered for the fitting exercise. As shown in Fig. 4.c, exponential and logarithmic models can be ruled out for obvious reasons. The obtained curvatures are incompatible with the experimental dataset. Moreover, for the exponential case, the number of events at the outset of the experiment is different from zero. For the logarithmic case, the number of events is negative at the outset. According to the results shown in Fig. 4.b and 4.c, PLP model offers the most acceptable representation of the available data.

4. Analysis of the power-law model

As shown in the previous Section, the PLP model ($\Lambda(t) = a{\cdot}t^b$) deserves special attention. It does not only provide a high correlation coefficient (R^2) but also always positive values for the number of events. Extracted parameters from Fig. 4.c are: $a = 5.4{\cdot}10^{-2}$ and $b = 1.6$ for the time expressed in seconds. In particular, $b > 1$ indicates reliability degeneration and an increasingly arrival rate of BD events with time. Later, we will show the effects of the opposite behavior. Being PLP a NHPP, the probability for a number k of events at time T can be calculated from:

$$P(N(T) = k) = \frac{a^k T^{bk}}{k!} exp\left[-aT^b\right] \quad (1)$$

so that the waiting time to the next event, given an event at time T, has

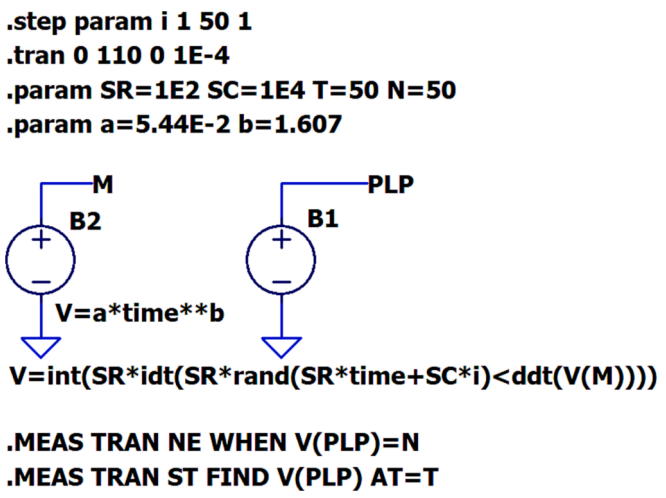

Fig. 6. LTSpice script for a PLP process. 50 curves are generated with identical model parameters. Model parameters are those reported in Fig. 4.c. Output M corresponds to the average number of events while output PLP to the corresponding stochastic result. For the sake of completeness, two measurement directives were included for the analysis.

the cumulative distribution function:

$$F_T(t) = 1 - exp\left\{ -a\left[(T+t)^b - T^b\right] \right\} \tag{2}$$

Expression (2) can be straightforwardly used for calculating the successive BD arrival times using the inversion algorithm described in Table 1. This approach is remarkably easy to implement in a spreadsheet. Simulation results obtained with this method are shown in Fig. 5.

TABLE 1. Inversion algorithm for the power-law model

Inversion algorithm for the power-law model	
1	**Input** exp. *data* and number of events *N*
2	Fit Eq. (2) to the exp. data to define a and b
3	define $t_{i-1} = 0$, $i = 0$
4	**for** $i < N$ then
5	generate u_i form Unif(0,1)
6	calculate $t_i = \left(t_{i-1}^b - \frac{1}{a}\ln(u_i)\right)^{\frac{1}{b}}$
7	define $t_{i-1} = t_i$
8	$i = i + 1$
9	**end**
10	**Output** $t_1, t_2, t_3, t_4, \ldots, t_N$

Interestingly, for PLP, the time-to-first BD ($T = 0$ in expression (2)) is Weibull-distributed which agrees with the weakest link character of oxide breakdown. Moreover, PLP is also consistent with the generation rate of defects in thin oxide films [4]. However, it is worth mentioning that though LSM provides reasonable parameter values, the method requires further confirmation. In this regard, parameter extraction can also be carried out using the maximum likelihood estimates (MLE). For time-truncated data, the PLP parameters read:

$$a = \frac{N}{t_N^b} \quad b = \frac{N}{\sum_{i=1}^{N} ln\left(\frac{t_N}{t_i}\right)} \tag{3}$$

In our case, $a = 3.4{\cdot}10^{-2}$ and $b = 1.7$ are obtained for $N = 83$ and $t_{83} = 88.1$ s, which closely agree with the extracted parameters using LSM. Notice that both the scale parameter a and shape parameter b depend on the last observed BD time so that they should be strictly treated as unknown random variables. However, as reported in [5], Bayesian estimates using the Higgins-Tsokos loss function can help to overcome this problem. In addition, the Cramér-von Mises goodness statistics can be used to identify whether the system strictly follows PLP or not. Confidence intervals for the parameter estimates are also provided in [6].

5. SPICE simulations of multiple BD events

In this Section, we pay particular attention to the generation of BD events in the framework of the LTspice simulator. Since a NHPP is assumed here for the generation process, the probability for the occurrence of a new BD event is simply given by the Poisson rule:

$$P(\Lambda(t+\Delta t) - \Lambda(t) = 1) = \lambda(t) \times \Delta t \tag{4}$$

where Δt is the time interval considered and λ the intensity of the process.

This generation rule can be expressed in LTspice as a rejection algorithm (see Fig. 6):

$$N(t) = int\{SR \times idt[SR \times rand(SR \times t + i) < ddt(\Lambda(t)))]\} \tag{5}$$

where *int* is the integer part of the number, *idt* the time integral, *ddt* the time derivative, *rand* the random number generator, and t the simulation time. SR is the sampling rate and i the random number generator seed. *rand*(SR·t + i) in (5) generates SR uniformly distributed random numbers in the range [0,1] per second. The index i shifts the argument of the function for every simulation run. *ddt*(Λ)/SR comes from the PLP process, Eqn. (4). When the logic expression < is true, a unity is added to the integral counter represented by *idt*. Now, this counter value times SR scales the number of events to the expected value. Fig. 7.a-c show the results obtained with the LTspice simulator. Fig. 7.a shows the stochastic process as well as its average trend, Fig. 7.b the time required to reach N BD events (ST) as a function of the simulation run and the number of events generated at time T (NE), and Fig. 7.c the shape of the stochastic paths around the average curve. This latter plot provides information about the evolution of the dispersion of the generated characteristics when the average trend is eliminated (detrended time series). Just for comparison, we have included a second generation model (not related to our devices) in order to demonstrate the flexibility of the proposed approach. The model considered is:

$$\Lambda(t) = a \times [1 - \exp(-b \times t)] \tag{6}$$

which expresses a self-saturation process with amplitude a and generation rate b. The corresponding results obtained with $a = 100$ and $b = 0.05$ are illustrated in Fig. 7.d-f. This process is typical of a first-order rate equation with limited number of events.

6. Conclusions

The generation of breakdown events in thin insulating layers (Al_2O_3) was investigated. Different standard reliability growth models were evaluated and discussed. The best option compatible with the experimental data seems to be the Power-law Poisson process. We have also shown how to calculate the successive breakdown times using two alternative approaches: inversion of the cumulative distribution function (more appropriate for spreedsheet calculators) and the rejection method (suitable for circuit simulators). We also discussed how the rejection method can be easily applied to other reliability growth models representing different failure mechanisms.

Declaration of Competing Interest

The authors declare the following financial interests/personal relationships which may be considered as potential competing interests: Enrique Miranda reports financial support was provided by European Metrology Programme for Innovation and Research (EMPIR).

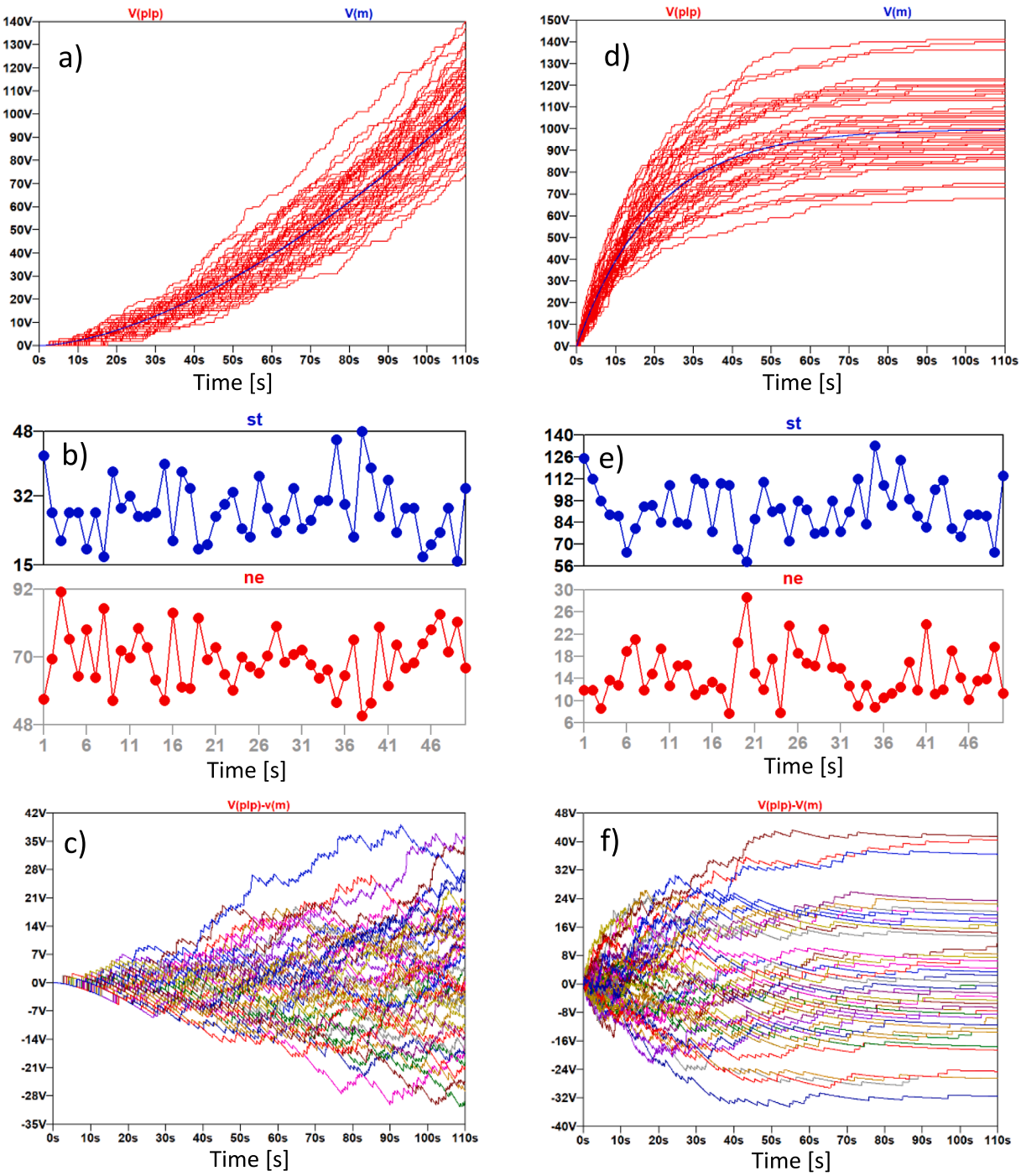

Fig. 7. a) and d): number of generated events using the plp and self-saturation processes, respectively. b) and e): results from the measurement directives, st: time-to-50 events, ne: number of events at 50 s. c) and f): Stochastic paths around the average trend calculated as V(PLP)-V(M), see Fig. 6.

Data availability

The authors do not have permission to share data.

Acknowledgements

E.M. and J.S. acknowledge the support provided by the European project MEMQuD, code 20FUN06, which has received funding from the EMPIR programme co-financed by the Participating States and from the European Union's Horizon 2020 research and innovation programme. The authors also thank projects 20225AT012 from CSIC, PID2022-139586NB-C41 and PID2022-139586NB-C42 from the Ministerio de Ciencia e Innovación, Spain. M.B.G. acknowledges the Ramón y Cajal grant No. RYC2020-030150-I. E.S acknowledges the Departament de Recerca i Universitats de la Generalitat de Catalunya for the 2020 FISDU 00261 scholarship.

References

[1] Muñoz J, et al. IEEE EDL 2020;41:1770–3.
[2] Jokiel-Rokita A, et al. in *Selected Stochastic Models in Reliability*. Kapital Ludzki 2021.
[3] Campabadal F, et al. J Vac Sci Technol B 2011;29.
[4] Conde A, et al. Solid St Electron 2012;71:48–52.
[5] F. Alenezi *et al.*, DOI:10.48550/arXiv.2002.00351.
[6] J. Chumnaul. Theses and Dissertations 2700 (2019). Mississippi State University.